Extreme Mechanics Letters 35 (2020) 100617

Contents lists available at ScienceDirect

Extreme Mechanics Letters

journal homepage: www.elsevier.com/locate/eml

The effect of water content on the elastic modulus and fracture energy of hydrogel

Ziqian Li [a], Zishun Liu [a,*], Teng Yong Ng [b], Pradeep Sharma [c]

[a] International Center for Applied Mechanics, State Key Laboratory for Strength and Vibration of Mechanical Structures, School of Aerospace Engineering, Xi'an Jiaotong University, Xi'an 710049, China
[b] School of Mechanical and Aerospace Engineering, Nanyang Technological University, 50 Nanyang Avenue, Singapore 639798, Singapore
[c] Department of Mechanical Engineering, University of Houston, USA

ARTICLE INFO

Article history:
Received 21 October 2019
Received in revised form 26 November 2019
Accepted 3 December 2019
Available online 5 December 2019

Keywords:
Scaling law
Polymer fraction
Elastic modulus
Fracture threshold

ABSTRACT

Both elastic and fracture behavior of hydrogel are affected by its water content. As shown by extensive experimental data, currently prevalent models, which are primarily based on the Flory–Rehner theory (F–R theory), are unable to correctly capture the effect of water content (or conversely polymer fraction) on the elastic modulus of hydrogels. Lake–Thomas theory cannot provide correct predictions on fracture toughness with different water content conditions as well. In this work, we carry out experiments on polyacrylamide (PAAm) gel and discover scaling-laws that differ significantly in the swollen and dehydrated state in addition to contradicting F–R model. We also derive scaling laws that are consistent with our experiments. Intriguingly, we find that the application of the scaling theory to fracture problems of the hydrogel can also provide a better theoretical prediction. An intriguing implication of this result is that the study of the fracture threshold of soft matter may be replaced to some extent by merely the studying of their elastic modulus.

1. Introduction

Well-designed hydrogels can exhibit several superior attributes such as high stretchability, biocompatibility, self-healing, improved ionic conductivity and more. They are expected to pave the way for future applications that range from drug delivery, flexible electronics, tissue engineering to optics. In most of the applications, hydrogels are likely to be subjected to complex periodical mechanic loads. The swelling and deswelling process that involves a gain and loss in water content respectively, in response to environmental changes is an example of the mechanical deformation experienced by hydrogels. Predicting the mechanical response of hydrogels in response to different environmental stimuli is, therefore, a fundamental problem underlying the design and use of hydrogels [1–10].

Arguably the most well-known model that describes the homogeneous swelling behavior of strained and undeformed polymers is F–R model [11]. This approach is based on the classical Gaussian chain model that describes the elastic response of a polymer network, as well as the mixing energy between polymer molecules and solvent molecules derived from Flory–Huggins solution theory [11–14]. Although it is widely used as the theoretical basis for interpreting the mechanical properties of swollen polymers [9] [15–19], F–R model suffers from several shortcomings which we highlight below.

Hydrogels become harder and more brittle during water loss, and vice-versa. According to F–R model, the elastic modulus E of hydrogels is proportional to the 1/3 power of the polymer volume fraction ϕ, i.e. $E(\phi) = E_0\phi^{1/3}$, where E_0 is the elastic modulus of the hydrogel in a dry state [20]. However, $E(\phi) = E_0\phi^{v}$ has various scaling exponents v as reported in some previous works, depending on the underlying elastomer network used to form a hydrogel [21,22]. Furthermore (as will be further elaborated in due course) our own experiments on PAAm hydrogels confirm that the scaling exponent v is not universally 1/3. Taking into consideration this discrepancy in the prediction of the scaling exponent by F–R model and experimental data, several phenomenological models have been proposed [21] [23–25]. The typical approach is to introduce a modified strain energy function beyond the standard Neo-Hookean model, by introducing additional phenomenological parameters. The key observation in this regard is that these phenomenological parameters are not universal, as most of them essentially amend the Neo-Hookean model to describe the mechanical response and one or more pertinent fitting parameters are then determined by experiments.

In this work, based on a scaling theory by de Gennes [26], which is often used to analyze the physical properties of long flexible chains, we establish a model to understand the swelling and deswelling behavior of hydrogels regarding its elastic response

* Corresponding author.
E-mail address: zishunliu@mail.xjtu.edu.cn (Z. Liu).

https://doi.org/10.1016/j.eml.2019.100617
2352-4316/

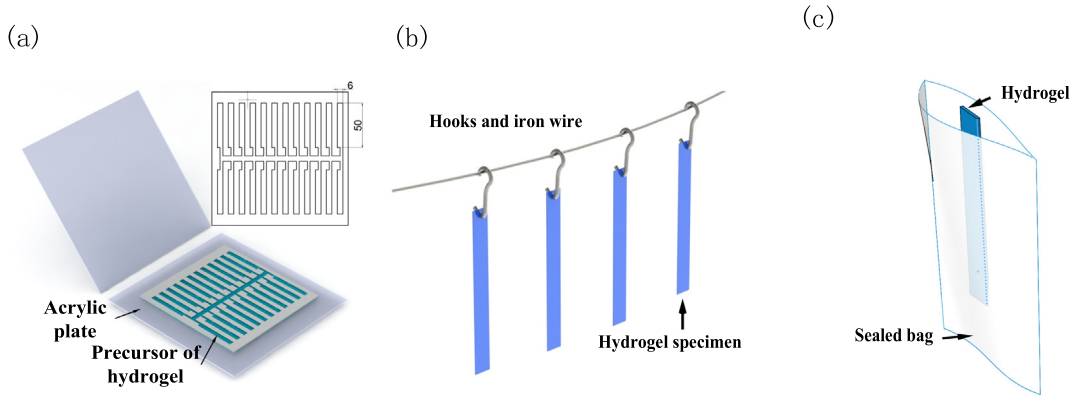

Fig. 1. (a) The acrylic plate mold for making hydrogel specimens (b) Hydrogel specimens are hung up for dehydration. (c) Hydrogel specimen placed into a sealed bag for approximately 3 days to allow for homogenization.

and fracture energy. Numerous studies over the years have used c' approach to analyze the mechanical behavior of polymers with satisfactory results [27–31]. We examined PAAm gel in the experiments. The scaling theory can successfully explain the various scaling exponents observed in our tests.

Furthermore, we postulate that the elastic modulus and fracture toughness of hydrogels are equivalent to some extent, because these two material properties both increase with the decrease of water content and vice-versa. Recently, Zhang et al. [32] tested the modulus and the fracture threshold of PAAm gel with different water content, and their results appear to verify this hypothesis. This provides some credence to our conjecture that there must be a connection between modulus and the fracture threshold of hydrogels. Based on this notion, we arrive at an expression for the fracture threshold that is similar to that for the modulus, thus yielding an elegant mathematical bridge between modulus and fracture threshold of hydrogels. Finally, a more accurate model to theoretically predict the fracture threshold of PAAm gel under different water content conditions is proposed.

The layout of this paper is as follows. Section 2 details the experimental processes and the data obtained. Section 3 provides the detailed derivations of the scaling-law between the modulus and polymer fraction. In Section 4, we propose the scaling theory to the study of fracture properties of PAAm gel and achieve better consistency with experimental data. Finally, we summarize all the major conclusions in Section 5.

2. Experimental section

We examined PAAm gel in this work. 20 wt.% powder of acrylamide is dissolved in deionized water. Irgacure 2959, 0.2 wt.%, and N, N-methylenebisacrylamide (MBAA), 0.02 wt.%, are added in acrylamide aqueous solution as photoinitiator and crosslinker, respectively [33]. The precursor solution of PAAm gel can become homogeneous very quickly. The liquid precursor solution is then poured into an acrylic plate mold (Fig. 1a) with 24 rectangular cells (50 mm × 6 mm size for each cell). The hydrogel precursor is cured under ultraviolet light (40 W power and 254 nm wavelength) for 4 h at room temperature.

To obtain hydrogel test-pieces with various water contents ranging from a swollen state to a deswollen state, a batch of cured hydrogel specimens from the mold is divided into two groups. The first group is the dehydrated group (low water content). Specimens are hung up for natural evaporation on a thin iron wire (Fig. 1b) and then sealed into plastic bags (Fig. 1c) at every half-hour interval. The other group is the water-absorption group. Specimens are soaked in water for swelling and then seal up one by one in sealed bags in every 5 min. It is necessary to seal

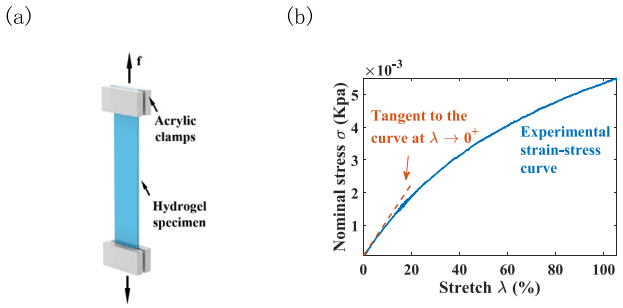

Fig. 2. Uniaxial tensile test for measuring the modulus of a hydrogel test-piece. (a) Schematic of a hydrogel test-piece (b) Nominal stress–stretch curve (elastic modulus of the hydrogel test-piece in the undeformed state is selected as the slope of the curve at $\lambda \to 0^+$).

those specimens for at least three days for complete homogenization [32]. Following these processes, we can eventually produce PAAm gel specimens with various water content ranging from approximately 30 wt.% to 95 wt.%.

The elastic modulus E of a PAAm gel test-piece is determined by uniaxial tensile testing. Four small acrylic clamps (Fig. 2a) are adhered to the two ends of a test-piece for securing it firmly to the clamps of the stretch machine (SHIMADZU AGS-X). The stretching rate is 5 mm/min which is sufficiently slow to avoid any possible dynamic effects from the test-pieces. Before conducting the uniaxial tensile test for a specimen, the mass m and its size (l × w × t) needs to be recorded. It is necessary to finish one tensile test as soon as possible to prevent the test-piece from losing too much water. The stretching machine can output the applied displacement L and corresponding force f, and based on them we can calculate the stretch ($\lambda = L/l$) and nominal stress ($s = f/wt$), and subsequently, draw the stretch–stress curve (Fig. 2b) for each test-piece. The slope of the stretch–stress curve at $\lambda \to 0^+$ determines the elastic modulus E of the hydrogel test-piece in the undeformed state.

Finally, we need to put those already tested sample pieces into an oven (80 °C) for complete dehydration. From weighing their dry mass m_{dry}, the corresponding polymer fractions by weight ψ are determined by $\psi = m_{dry}/m$. However, we will use polymer fraction by volume ϕ in following theory sections, which is the hydrogel's volume in the dry state divided by the volume before the test ($\phi = V_{dry}/V$). Over 99 wt.% components of the hydrogels used in Section 2 are acrylamide and water. The density of acrylamide ρ_A is 1.13 g/cm^3 and the water density ρ_w is 1 g/cm^3. Thus, we have $\phi = 1/\left[\left(\psi^{-1} - 1\right)(\rho_A/\rho_w) + 1\right]$. Eventually, the

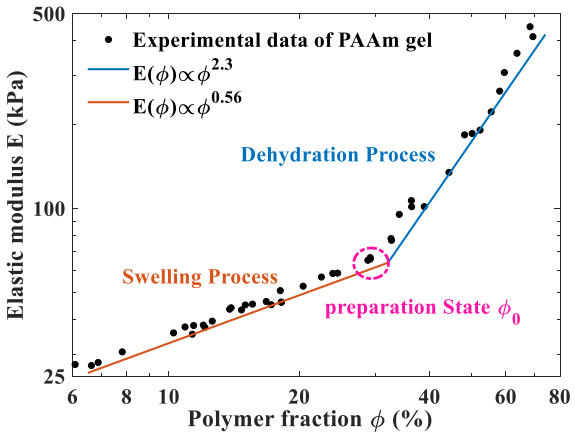

Fig. 3. The log–log plot between polymer fraction ϕ and elastic modulus $E(\phi)$ of PAAm gel, the scaling exponent in the swelling process is 0.56, which is smaller than the one in the dehydration process, 2.3.

graph of $\phi \sim E$ discrete data is obtained by measuring dozens of specimens as shown in Fig. 3.

We also notice that the water content of specimens in the preparation state, obtained by the air-drying method, decreases to some extent. The water content of a PAAm gel specimen that is just taken out from the casting model should be 80 wt.%. However, after entirely desiccating (at 25 °C, 60 °C or even 80 °C) the specimens of PAAm that are just cured, their water contents (loss mass divided by initial mass) unexpectedly decrease slightly to around 72 wt.%. This discrepancy of water content might be attributed to the different water structures in the hydrogel network. These structures can be classified into three categories: bound water, intermedia water, and free water [34–37]. We conjecture that only free and intermedia water can escape from a network by natural evaporation, while bound water will stay in the system due to its strong interconnection with polymer chains. Consequently, the polymer mass will be overestimated as the mass of bound water is inevitably included.

3. Scaling-law theory for hydrogel modulus with water content change

We shall denote ϕ_0 as the polymer fraction in the preparation state, where cross-linkage junctions have not formed in a hydrogel precursor solution, and the corresponding volume is V_0. It is evident that $V_0\phi_0 = V\phi = V_{dry}$ because of incompressibility. When a hydrogel specimen swells in water under the unconstrained state, it deforms uniformly by the same amount in all directions. Hence the stretch ratio λ in each direction is

$$\lambda = (V/V_0)^{1/3} = (\phi_0/\phi)^{1/3} \tag{1}$$

The elastic energy F_{el} of a polymer chain adopts Panyukov form in Eq. (2) [38,39], which is the modern treatment of polymer networks utilizing a more general form for the elastic energy of a swollen or deformed network strand.

$$F_{el} \approx kT(\lambda R_0)^2/R_{ref}^2 \tag{2}$$

where R_0 is the mean-square end-to-end distance of network strands in their preparation state, and R_{ref}^2 is the mean-square fluctuation of the end-to-end distance of the network strand. In many cases, R_{ref}^2 is equal to the mean-square end-to-end distance of a free chain which is in the same precursor solution that the cured hydrogel has [11]. Its expression, as given by Eq. (A.3) in the Appendix, is

$$R_{ref} \sim \phi^{-(\upsilon-1/2)/(3\upsilon-1)} \tag{3}$$

where υ is defined in Eq. (A.1). In scaling theory, the shear modulus G of the gel in is proportional to the product of the chain number density υ and the elastic free energy per chain F_{el} [11].

$$G(\phi) \approx \upsilon \cdot F_{el} \tag{4}$$

The chain number density $\upsilon = n/NV$ can be easily determined, where $n = V_{dry}/v_e$ is the total number of monomers within the polymer network, and $v_e \cong a^3$ is the volume of one monomer (a is Kuhn length defined in Appendix). In the case of incompressible materials, $E = 3G$. Eq. (4) can be $E(\phi) \approx \phi \cdot F_{el}$. Then, the chain number density can be expressed as $\upsilon \cong \phi/(Na^3)$. Consequently,

$$E(\phi) \approx kT\frac{\phi}{Na^3}\frac{(\lambda R_0)^2}{R_{ref}^2} \tag{5}$$

We can use Eqs. (1) to (5) to draw some preliminary inferences. Firstly, the network strands will increase the elastic modulus during swelling (E changes with $\phi^{-2/3}$), while the decreasing of chain number density υ caused by swelling leads to the reduction of the modulus [see Eq. (4)]. Hence, the net effect is that the gel modulus will slightly decrease during swelling. Secondly, it is impossible to produce a negative stretch in the process of dehydration. Thus, only the chain number density υ can increase the modulus. The statements above imply that the scaling exponent during swelling is smaller than that in the dehydration process. PAAm gel has smaller scaling exponents in the swelling state than that in the deswelling state. In the following two subsections, we will give much-detailed interpretations concerned with Fig. 3.

3.1. From preparation state to swelling state

The elasticity is balanced by the osmotic pressure π of a semidilute solution of uncrosslinked chains at the same concentration ($G \sim \pi$). The osmotic pressure π stays unchanged during the formation of the crosslink junctions. Therefore, the elastic modulus of a hydrogel in preparation state ϕ_0 is balanced with osmotic pressure. Moreover, the end-to-end distance R_0 of a network strand in the preparation state can be calculated based on ϕ_0, and it is given by Eq. (A.3) [11].

$$R_0 \approx \phi_0^{-(\upsilon-1/2)/(3\upsilon-1)} \tag{6}$$

During swelling, many new water molecules (small purple circles in Fig. 4) have diffused into the PAAm network, and the cross-linkage junctions (red points) of the hydrogel networks have moved further apart. As a result, chains will be stretched to some extent due to the volume expanding, and the system will store some elastic energy. Therefore, the network strands are no longer in the unconstrained state but in a stretched state. In such case, the end-to-end distance become R_{ref} [see Eq, (3)] rather than R_0. Here, ϕ_0 is uncoupled with ϕ, and elastic modulus G is not balanced with osmotic pressure π.

For PAAm in the swelling state, by substituting the Eqs. (1), (3) and (6) into Eq. (5), we have

$$E(\phi) \approx \frac{kT}{Na^3}\phi_0^{1/[3(3\upsilon-1)]}\phi^{(9\upsilon-4)/[3(3\upsilon-1)]} \tag{7}$$

Since $\upsilon = 0.588$ (the theoretical value derived by the renormalization group method [40]), the elastic modulus of a PAAm gel in the swelling state ($\phi < \phi_0$) increases slightly as $E(\phi) \sim \phi^{0.56}$, which is very close to the red line in Fig. 3.

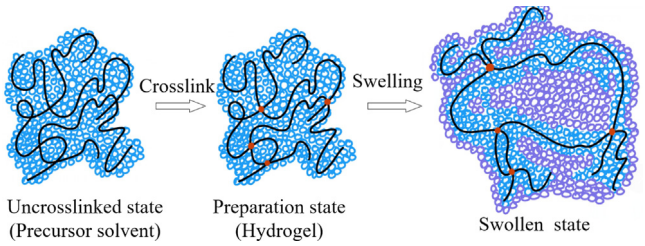

Fig. 4. Schematic diagram of crosslinking and swelling process of hydrogels. The crosslinking process only forms crosslink junctions with any other features that stay unchanged. The swelling of hydrogel will move crosslink junctions apart and stretch hydrogel chains a bit.

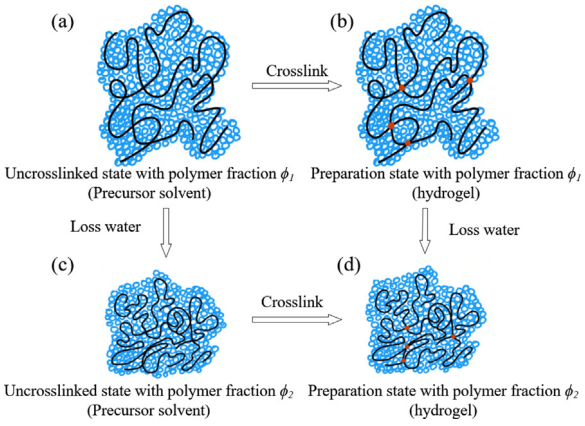

Fig. 5. The osmotic pressure stays constant in the process of forming crosslink points. Process (a)→(b)→(d) is equivalent to Process (a)→(c)→(d).

3.2. From preparation state to dehydration state

In the dehydration process, the scaling exponent is different. Unlike the conditions in Section 3.1, the network strands become denser, however, they still preserve the unconstrained state during dehydration. There is no elastic energy stored in the system. Therefore, we have two ways to obtain a hydrogel network with polymer fraction ϕ_2 (as shown in Fig. 5d) from the precursor solvent with polymer fraction ϕ_1 (Fig. 5a): ①, forming crosslink junctions first and then losing some water (along the path of Fig. 5a→8b→8d); ②, loss water first and then forming crosslink junctions (along the path of Fig. 5a→8c→8d). By these two ways, the final osmotic pressures are identical as the concentrations are the same, however, R_0 is not equal as R_0 depends on the network configuration at the moment of forming gel [see Eq. (A.3)].

As mentioned before, the elasticity is balanced by the osmotic pressure π of uncrosslinked chains at the same concentration ($G \sim \pi$). Here, we can directly use this scaling-law to obtain the correlation between E and ϕ. The expression of the equilibrium state of a gel can be determined by Eq. (A.5). The modulus can also be expressed as

$$E \cong G \sim \pi \cong \frac{kT}{a^3}\left(\frac{v_e}{a^3}\right)^{3(2v-1)/(3v-1)} \phi^{3v/(3v-1)} \tag{8}$$

$$E(\phi) \approx \phi^{3v/3v-1} \tag{9}$$

Since $v = 0.588$, the elastic modulus of an AAm gel in the dehydration state increases significantly with $E(\phi) \sim \phi^{2.3}$ (the blue line in Fig. 3).

4. Scaling theory of hydrogel fracture threshold

The threshold for fatigue fracture Γ_0 (fracture threshold for short) of rubber has been described by the Lake–Thomas model, in which C–C bonds will break ahead of the crack tip during crack propagation [41]. Basing on Lake–Thomas mode, Zhang et al. have proposed that the fracture threshold Γ_0 of a PAAm gel will increase slowly with water content reduction, as $\Gamma_0 \sim \phi^{2/3}$ [32]. Earlier, Creton and Ciccotti had proposed another relation $\Gamma_0 \sim \phi$ [42]. However, both of them are unable to accurately predict the relationship between fracture threshold and polymer fraction. According to Lake–Thomas model, at the crack tip, some chains span the plane of crack propagation, and the fracture threshold Γ_0 is the product of the number of such chains per cross-sectional area (ϑ) and the energy required to break one bridging strand (U) [43].

$$\Gamma_0(\phi) = \vartheta \cdot U \tag{10}$$

ϑ has a relation with the bulk chain density v. If L is the thickness of the single bridging-chain layer, then within a unit area, the number of chains is vL. Thus, we can obtain the relation $\vartheta = vL$, which can also be expressed as $\vartheta \cong v$ in scaling law. The energy for breaking a chain U is provided by external forces. The put-in energy will store in elastic energy first. Then, at the break moment, the put-in energy reaches the critical value U of every chain. Thus, when crack tip just begins to propagate, F_{el} can be seen as equal to U. In scaling law, it can be expressed as $U \cong F_{el}$. Therefore, Eq. (10) becomes

$$\Gamma_0(\phi) \cong v \cdot F_{el} \tag{11}$$

It is fascinating that Eqs. (11) and (4) have the same expression. Consequently, we can use a similar method in Section 3 to derive the relation between Γ_0 and ϕ. Since the hydrogel network strands are highly stretched at the crack tip, we assume that the strands will break as the stretch ratio at the crack tip reaches a critical value λ_c. This critical value is assumed to be the product of the stretch ratio λ_s caused by expansion/shrinking of volume and the stretch ratio λ_f caused by put-in energy such as external stretch force ($\lambda_c = \lambda_s\lambda_f$). The exact value of λ_c is not known explicitly, and it may vary depending on the loading method. Tang et al. applied monotonic, static, and cyclic load on PAAm gel and observed three types of fracture behavior: fast fracture, delayed fracture, and fatigue fracture. As different fracture behaviors have different fracture critical values [44], we need to assume that the strands will break as the stretch ratio at the crack tip reaches a critical value λ_c, only in the loading situation corresponding to λ_c. Substituting λ_c into Eq. (5) then, we have

$$\Gamma_0(\phi) \approx \frac{kT}{a^3}\frac{\phi}{N}\frac{(\lambda_c R_0)^2}{R_{ref}^2} \tag{12}$$

Substituting $\lambda_c = \lambda_s\lambda_f$ to Eq. (12), we obtain

$$\Gamma_0(\phi) \approx \lambda_f^2\frac{kT}{a^3}\frac{\phi}{N}\frac{(\lambda_s R_0)^2}{R_{ref}^2} \tag{13}$$

The only difference between. Eqs. (13) and (5) is that Eq. (13) has an extra λ_f^2. Since λ_f is induced by external forces rather than swelling/deswelling process, λ_f is independent of ϕ. Here, we are only interested in the correlation between ϕ and Γ_0. Therefore, λ_f can be ignored in the scaling-law theory.

$$\Gamma_0(\phi) \approx \frac{kT}{a^3}\frac{\phi}{N}\frac{(\lambda_s R_0)^2}{R_{ref}^2} \tag{14}$$

Eqs. (14) and (5) are now exactly the same. By using the same method as in Section 3, the relationship between Γ_0 and ϕ is also defined as

$$\Gamma_0(\phi) \sim \phi^{(9v-4)/[3(3v-1)]} \quad \text{for } \phi < \phi_0 \tag{15}$$

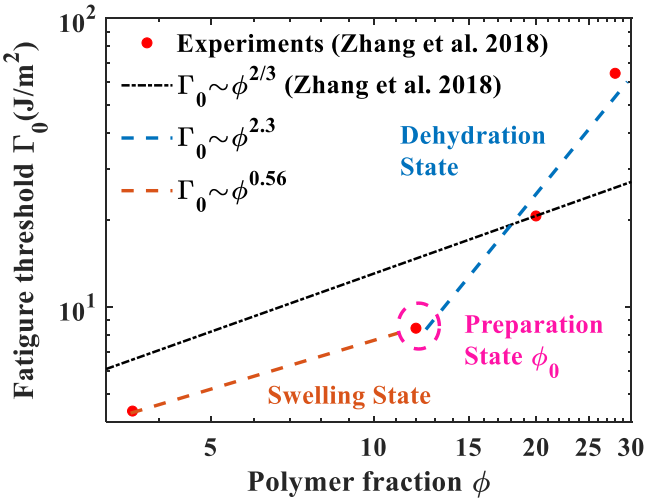

Fig. 6. The log–log plot between polymer fraction ϕ and fatigue threshold Γ_0 of PAAm hydrogel. Experimental data and the theoretical prediction (black dash line) are from Zhang et al. [32]. Our theory gives a better prediction: in the swelling process, the threshold decreases slightly with decreasing of polymer fraction, $\Gamma_0 \sim \phi^{0.56}$ (orange dash line); in the dehydration process, the scaling exponent is larger, $\Gamma_0 \sim \phi^{2.3}$ (blue dash line). The intersection of the two trends happens to occur at $\phi = \phi_0$. (For interpretation of the references to color in this figure legend, the reader is referred to the web version of this article.)

and

$$\Gamma_0(\phi) \sim \phi^{3\upsilon/(3\upsilon-1)} \quad \text{for } \phi > \phi_0 \tag{16}$$

For PAAm gel, the polymer solution belongs to the good solvent. Substituting $\upsilon = 0.588$ to Eqs. (15) and (16), we have $\Gamma_0(\phi) \sim \phi^{0.56}$ for $\phi < \phi_0$ and $\Gamma_0(\phi) \sim \phi^{2.3}$ for $\phi > \phi_0$. Referring to the experimental data of Zhang et al. [32]. Fig. 6 which shows our theoretical results, to our surprise, is fully consistent with their reported experimental data much better than their own theatrical prediction. The original literature of Zhang et al. only tested the fracture thresholds of PAAm gels under four different water contents and did not draw error bars either. The point enclosed by the dash-line ellipse in Fig. 6 is the test result of PAAm gels under preparation state (87 wt.% water content) in their original paper. They only tested swollen PAAm gels with 96 wt.% water content and just produced two types of dehydrated PAAm gels (78 wt.% and 69 wt.% water content) by a similar air-drying method. They were only able to provide experimental data for four sorts of PAAm gels because fatigue tests for hydrogels are usually very time-consuming. If we want to obtain more experimental data to verify our theoretical results on PAAm gel's fracture threshold, at least hundreds of fatigue tests with various water contents should be done. No work has provided such tremendous data so far.

Our scaling theory can only treat nearly perfectly elastic polymer like PAAm gel for the moment because we previously use an assumption that U is approximately proportional to F_{el} ($U \sim F_{el}$) up to a dimensional constant. Only a perfectly elastic hydrogel can release all elastic energy F_{el} for crack propagation, while hydrogels possessing viscoelasticity, such as double-network gels, can dissipate more or less F_{el}. Under such circumstance, U cannot be simply assumed to be approximately proportional to F_{el} any more because viscoelasticity is a nonlinear behavior.

5. Concluding remarks

Hydrogels are a class of polymeric materials that comprise the polymer network and solvent molecules. F–R model, based on mean-field assumptions, has several limitations and it is unable to accurately predict the variation of the elastic modulus with respect to the water content. In the current work, we successfully use the scaling-law theory that can accurately capture the scaling relation between elastic modulus and polymer fraction of PAAm gel. For $\phi > \phi_0$, $E(\phi) \sim \phi^{2.3}$, and for $\phi < \phi_0$, $E(\phi) \sim \phi^{0.56}$. Subsequently, we conducted experiments and verified the theory. The results show that the scaling exponents are generally different in the swelling and deswelling processes in a hydrogel.

Furthermore, we discover a rather straightforward but intriguing connection between modulus and fracture threshold of PAAm gel. It is motivated by the well-known observation that the hydrogel becomes hard and more brittle during the deswelling process, and vice versa. In particular, we can establish scaling-laws for the fracture properties of PAAm gel, viz: that $\Gamma_0(\phi) \sim \phi^{2.3}$ for $\phi > \phi_0$, and $\Gamma_0(\phi) \sim \phi^{0.56}$ for $\phi < \phi_0$. This result is consistent with experimental data reported by Zhang et al. [32]. We believe that the establishment of this connection between fracture threshold and elastic modulus of hydrogels is significant as it implies that the study of the fracture threshold of soft matter can be replaced to some extent by the study of their elastic modulus.

Declaration of competing interest

The authors declare that they have no known competing financial interests or personal relationships that could have appeared to influence the work reported in this paper.

Acknowledgments

Ziqian Li and Zishun Liu are grateful for the support from the National Natural Science Foundation of China through grant numbers 11572236 and 11811530287.

Appendix

We will introduce and explicitly define some mathematical signs and essential physical concepts in the scaling-law theory used in this paper, even as more details can be obtained from the book [11]. Scaling theory eliminates the barrier between unintelligible statistical data and rigorous theoretical formulas as numerical coefficients in scaling theory are ignored in most formulas. In scaling theory, the sign "≅" indicates a numerical approximation, the sign "≈" indicates that two quantities are proportional to each other up to a dimensionless prefactor of order unity, and the notation "∼" indicates that the two quantities are proportional to each other up to a dimensional constant.

The difference between an ideal chain and a real chain in polymer science is that the former follows a random walk model, while the latter is derived from the self-avoiding walk model. Self-avoiding walk model indicates that monomers on a real chain can exclude somewhat volume $v_e \approx a^3$, and a is called Kuhn length of polymer chains [12]. Besides, an isolated polymer chain can be regarded as a fractal structure which possesses self-similar property, as shown in Fig. A.1a, in which the small blob is called thermal blob and its size marked as ξ_T. The blob each corresponds to the length scale $\xi_T \approx a^4/|v_e|$ at which the interaction energy is of the order of the thermal energy kT. On smaller scales the interaction is negligible, and the chain behaves like a real chain. On length scales larger than the blob size ξ_T, the interaction energy is larger than kT and conformations of a polymer chain are controlled by interaction effects.

The end-to-end distance of a polymer chain (R) in athermal and good solvents is determined by [11]

$$R \approx a\left(\frac{v_e}{a^3}\right)^{2\upsilon-1} N^{\upsilon} \tag{A.1}$$

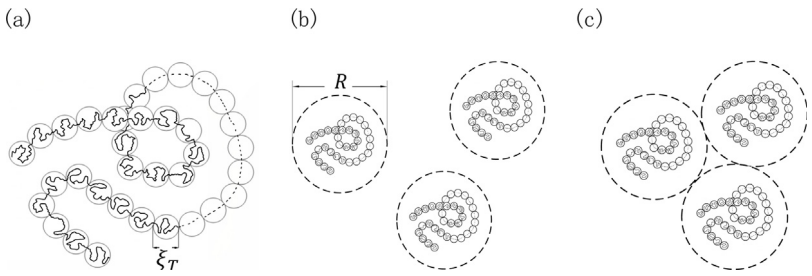

Fig. A.1. (a) Schematic diagram of thermal blob model of the polymer chain (The blob size is ξ_T). The distribution of polymer chain in (b) dilute polymer solution and in (c) overlap concentration ϕ^*.

where v is the scaling exponent, Flory gave $v = 0.6$ by using mean-field theory, but more sophisticated theories lead to a more accurate estimate of the scaling exponent in three dimensions, $v = 0.588$ [40]. In polymer solvent, polymer coils are far from each other and behave as isolated real chains at low concentrations (Fig. A.1b). When the volume fraction of polymer ϕ exceeds the volume fraction of monomers inside each isolated coil, polymer chains begin to overlap each other. In this case, the current concentration of the solvent is called the overlap concentration ϕ^* (Fig. A.1c). Concentration c and volume fraction ϕ are not completely equivalent in the physical meaning, but they have $c \sim \phi$ in scaling theory. Hence, it is rational to replace c with ϕ.

$$\phi^* \approx \frac{Na^3}{R^3} = \left(\frac{a^3}{v_e}\right)^{6v-3} N^{1-3v} \tag{A.2}$$

Only when the polymer fraction in precursor (ϕ_0) is larger than ϕ^* is it possible to form a hydrogel network by crosslinking. At higher polymer fraction ($\phi_0 > \phi^*$), chains interpenetrate and the solution is called semidilute.

There is a critical concept in a semidilute solution called correlation length ξ. On length scales smaller than the correlation length, the conformations of a chain are very similar to that in a dilute solution with a solvent of the same quality. On length scales larger than the correlation length, the excluded volume interactions are screened by the overlapping chains, which is called screen-effect in polymer science. The polymer fraction dependence of polymer size R in semi-dilute solution is [11]

$$R \approx a\left(\frac{v_e}{a^3\phi}\right)^{(v-1/2)/(3v-1)} N^{1/2} \quad \text{for } (\phi^* < \phi) \tag{A.3}$$

The correlation length ξ is also influenced by polymer fraction ϕ. The correlation length ξ decreases with increasing concentration, but the size of a thermal blob ξ_T is independent of concentration. Therefore, at some concentration $\phi^{**} \approx v_e/a^3$, the correlation length ξ is equal to the thermal blob ξ_T. It is the boundary between the semidilute regime and the concentrated solution regime. At and above the concentration ($\phi > \phi^{**}$), polymer chains are ideal ($R \approx N^{1/2}a$). In dilute regime ($\phi < \phi^*$), thermal blobs are isolated each other and chains are ideal as well. Only in the semidilute regime ($\phi^* < \phi < \phi^{**}$), the size of a polymer chain follows Eq. (A.1). The concentration ϕ dependence of the polymer size R in the semidilute solution can be rewritten with ϕ^{**} [11].

$$R \approx R_0\left(\frac{\phi}{\phi^{**}}\right)^{-(v-1/2)/(3v-1)} \quad \text{for } (\phi^* < \phi < \phi^{**}) \tag{A.4}$$

Flory and Huggins have proposed the expression of osmotic pressure π by using mean-field theory. The mean-field theory correctly predicts that the osmotic pressure is independent of molar mass in semidilute solution. However, the mean-field theory fails to consider the correlations between monomers along the chain. De Gennes takes into account the correlations between monomers along the chain by using the scaling approach and derived the scaling connection between osmotic pressure π and polymer fraction ϕ [26]. The osmotic pressure π in a good and athermal solvent is [11]

$$\pi \cong \frac{kT}{a^3}\left(\frac{v_e}{a^3}\right)^{3(2v-1)/(3v-1)} \phi^{3v/(3v-1)} \tag{A.5}$$

References

[1] J. Hu, Y. Zhou, Z. Liu, The friction effect on buckling behavior of cellular structures under axial load, Int. J. Appl. Mech. 10 (2018) 1850013, http://dx.doi.org/10.1142/s1758825118500138.

[2] K.E. Arash, B. Mostafa, S. Hamid, F. Ghader, A combined analytical–numerical investigation on photosensitive hydrogel micro-valves, Int. J. Appl. Mech. 09 (2017) 1750103, http://dx.doi.org/10.1142/s1758825117501034.

[3] S. Xu, Z. Liu, A nonequilibrium thermodynamics approach to the transient properties of hydrogels, J. Mech. Phys. Solids 127 (2019) 94–110, http://dx.doi.org/10.1016/j.jmps.2019.03.008.

[4] C. Yi, X. Zhang, H. Yan, B. Jin, Finite element simulation and the application of amphoteric ph-sensitive hydrogel, Int. J. Appl. Mech. 09 (2017) 1750063, http://dx.doi.org/10.1142/s1758825117500636.

[5] Y. Zhang, L. Tang, B. Xie, K.J. Xu, Z. Liu, Y. Liu, J. Zhenyu, S. Dong, A variable mass meso-model for the mechanical and water-expelled behaviors of PVA hydrogel in compression, Int. J. Appl. Mech. 09 (2017) 1750044, http://dx.doi.org/10.1142/s1758825117500442.

[6] S. Zheng, Z. Li, Z. Liu, The fast homogeneous diffusion of hydrogel under different stimuli, Int. J. Mech. Sci. 137 (2018) 263–270, http://dx.doi.org/10.1016/j.ijmecsci.2018.01.029.

[7] S. Zheng, Z. Liu, Constitutive model of salt concentration-sensitive hydrogel, Mech. Mater. 136 (2019) 103092, http://dx.doi.org/10.1016/j.mechmat.2019.103092.

[8] Y. Zhou, J. Hu, Z. Liu, Deformation behavior of fiber-reinforced hydrogel structures, Int. J. Struct. Stab. Dyn. 19 (2019) 1950032, http://dx.doi.org/10.1142/S0219455419500329.

[9] Z. Liu, W. Toh, T.Y. Ng, Advances in mechanics of soft materials: A review of large deformation behavior of hydrogels, Int. J. Appl. Mech. 7 (2015) http://dx.doi.org/10.1142/s1758825115300011.

[10] S. Xu, S. Cai, Z. Liu, Thermal conductivity of polyacrylamide hydrogels at the nanoscale, ACS Appl. Mater. Interfaces 10 (2018) 36352–36360, http://dx.doi.org/10.1021/acsami.8b09891.

[11] M. Rubinstein, R.H. Colby, Polymer Physics, Oxford University Press, New York, 2003.

[12] W. Kuhn, Über die gestalt fadenförmiger moleküle in lösungen, Kolloid-Z. 68 (1934) 2–15, http://dx.doi.org/10.1007/bf01451681.

[13] P.J. Flory, J.R. Jr, Statistical mechanics of cross-linked polymer networks II swelling, J. Chem. Phys. 11 (1943) 521–526, http://dx.doi.org/10.1063/1.1723792.

[14] P.J. Flory, Principles of Polymer Chemistry, Cornell University Press, New York, 1953.

[15] W. Hong, Z. Liu, Z. Suo, Inhomogeneous swelling of a gel in equilibrium with a solvent and mechanical load, Int. J. Solids Struct. 46 (2009) 3282–3289, http://dx.doi.org/10.1016/j.ijsolstr.2009.04.022.

[16] M.K. Kang, R. Huang, Swell-induced surface instability of confined hydrogel layers on substrates, J. Mech. Phys. Solids 58 (2010) 1582–1598, http://dx.doi.org/10.1016/j.jmps.2010.07.008.

[17] J. Li, Y. Hu, J.J. Vlassak, Z. Suo, Experimental determination of equations of state for ideal elastomeric gels, Soft Matter 8 (2012) 8121–8128, http://dx.doi.org/10.1039/c2sm25437a.

[18] K. Michael C, P. Jonathan T, S. Stephanie D, P. Nicholas A, Stimulus-responsive hydrogels: Theory, modern advances, and applications, Mater. Sci. Eng.: R 93 (2015) 1–49, http://dx.doi.org/10.1016/j.mser.2015.04.001.
[19] S.A. Chester, L. Anand, A coupled theory of fluid permeation and large deformations for elastomeric materials, J. Mech. Phys. Solids 58 (2010) 1879–1906, http://dx.doi.org/10.1016/j.jmps.2010.07.020.
[20] L.R.G. Treloar, The Physics of Rubber Elasticity, third ed., Oxford University Press, New York, 1975, http://dx.doi.org/10.1063/1.3060678.
[21] D. Okumura, A. Kondo, N. Ohno, Using two scaling exponents to describe the mechanical properties of swollen elastomers, J. Mech. Phys. Solids 90 (2016) 61–76, http://dx.doi.org/10.1016/j.jmps.2016.02.017.
[22] K. Urayama, T. Kawamura, S. Kohjiya, Elastic modulus and equilibrium swelling of networks crosslinked by end-linking oligodimethylsiloxane at solution state, J. Chem. Phys. 105 (1996) 4833–4840, http://dx.doi.org/10.1063/1.472320.
[23] G.B. McKenna, K.M. Flynn, Y. Chen, Experiments on the elasticity of dry and swollen networks: implications for the frenkel-flory-rehner hypothesis, Macromolecules 22 (1989) 4507–4512, http://dx.doi.org/10.1021/ma00202a022.
[24] A.D. Drozdov, Constitutive equations in finite elasticity of swollen elastomers, Int. J. Solids Struct. 50 (2013) 1494–1504, http://dx.doi.org/10.1016/j.ijsolstr.2013.01.031.
[25] Y. Pan, Z. Zhong, Modeling of the mechanical degradation induced by moisture absorption in short natural fiber reinforced composites, Compos. Sci. Technol. 103 (2014) 22–27, http://dx.doi.org/10.1016/j.compscitech.2014.08.010.
[26] P.-G. De Gennes, Scaling Concepts in Polymer Physics, Cornell University Press, New York, 1979.
[27] S.P. Obukhov, M. Rubinstein, R.H. Colby, Network modulus and superelasticity, Macromolecules 27 (1994) 3191–3198, http://dx.doi.org/10.1021/ma00090a012.
[28] M. Rubinstein, R.H. Colby, A.V. Dobrynin, J.-F. Joanny, Elastic modulus and equilibrium swelling of polyelectrolyte gels, Macromolecules 29 (1996) 398–406, http://dx.doi.org/10.1021/ma9511917.
[29] M. Pütz, K. Kremer, R. Everaers, Self-similar chain conformations in polymer gels, Phys. Rev. Lett. 84 (2000) 298, http://dx.doi.org/10.1103/PhysRevLett.84.298.
[30] S. Kundu, A.J. Crosby, CaVitation and fracture behavior of polyacrylamide hydrogels, Soft Matter 5 (2009) 3963–3968, http://dx.doi.org/10.1039/b909237d.
[31] T. Sakai, M. Kurakazu, Y. Akagi, M. Shibayama, U. Chung, Effect of swelling and deswelling on the elasticity of polymer networks in the dilute to semi-dilute region, Soft Matter 8 (2012) 2730–2736, http://dx.doi.org/10.1039/c2sm07043j.
[32] E. Zhang, R. Bai, X. Pierre Morelle, Z. Suo, Fatigue fracture of nearly elastic hydrogels, Soft Matter 14 (2018) 3563–3571, http://dx.doi.org/10.1039/c8sm00460a.
[33] H. Yuk, T. Zhang, S. Lin, G.A. Parada, X. Zhao, Tough bonding of hydrogels to diverse non-porous surfaces, Nat. Mater. 15 (2016) 190–196, http://dx.doi.org/10.1038/nmat4463.
[34] M.N. Khalid, F. Agnely, N. Yagoubi, J.L. Grossiord, G. Couarraze, Water state characterization swelling behavior thermal and mechanical properties of chitosan based networks, Eur. J. Pharmaceut. Sci. 15 (2002) 425–432, http://dx.doi.org/10.1016/S0928-0987(02)00029-5.
[35] W. Li, F. Xue, R. Cheng, States of water in partially swollen poly(vinyl alcohol) hydrogels, Polymer 46 (2005) 12026–12031, http://dx.doi.org/10.1016/J.POLYMER.2005.09.016.
[36] T. Wang, S. Gunasekaran, State of water in chitosan-PVA hydrogel, J. Appl. Polym. Sci. (2006) http://dx.doi.org/10.1002/app.23526.
[37] V. Gun'ko, I. Savina, S. Mikhalovsky, Properties of water bound in hydrogels, Gels (2017) http://dx.doi.org/10.3390/gels3040037.
[38] S.V. Panyukov, Scaling theory of high elasticity, Sov. Phys. JETP 71 (1990) 372–379.
[39] S. Panyukov, Y. Rabin, Statistical physics of polymer gels, Phys. Rep. 269 (1996) 1–131.
[40] J. Zinn-Justin, Quantum Field Theory and Critical Phenomena, Clarendon Press, 1996.
[41] G.J. Lake, A.G. Thomas, The strength of highly elastic materials, Proc. R. Soc. Lond. A 300 (1967) 108–119, http://dx.doi.org/10.1098/rspa.1967.0160.
[42] C. Creton, M. Ciccotti, Fracture and adhesion of soft materials: a review, Rep. Prog. Phys. 79 (2016) 46601.
[43] S. Wang, S. Panyukov, M. Rubinstein, S.L. Craig, Quantitative adjustment to the molecular energy parameter in the lake–thomas theory of polymer fracture energy, Macromolecules 52 (2019) 2772–2777, http://dx.doi.org/10.1021/acs.macromol.8b02341.
[44] J. Tang, J. Li, J.J. Vlassak, Z. Suo, Fatigue fracture of hydrogels, Extreme Mech. Lett. (2017) http://dx.doi.org/10.1016/j.eml.2016.09.010.